### Title
Sunscreen enhancement of UV-induced reactive oxygen species in the skin




### Journal
Free Radical Biology and Medicine, 41(8)

### ISSN
0891-5849



### Authors
Hanson, Kerry M
Gratton, Enrico
Bardeen, Christopher J



### Publication Date
2006-10-01

### DOI
10.1016/j.freeradbiomed.2006.06.011

Available online at www.sciencedirect.com
ScienceDirect
Free Radical Biology & Medicine 41 (2006) 1205–1212
www.elsevier.com/locate/freeradbiomed

Original Contribution

# Sunscreen enhancement of UV-induced reactive oxygen species in the skin

Kerry M. Hanson [a,*], Enrico Gratton [b], Christopher J. Bardeen [a]

[a] *Department of Chemistry, University of California at Riverside, Riverside, CA 92506, USA*
[b] *Laboratory for Fluorescence Dynamics, Department of Bioengineering, University of California at Irvine, Irvine, CA 92697, USA*

Received 1 March 2006; revised 17 May 2006; accepted 14 June 2006
Available online 6 July 2006

**Abstract**

The number of UV-induced (20 mJ $cm^{-2}$) reactive oxygen species (ROS) generated in nucleated epidermis is dependent upon the length of time the UV filter octocrylene, octylmethoxycinnamate, or benzophenone-3 remains on the skin surface. Two-photon fluorescence images acquired immediately after application of each formulation (2 mg $cm^{-2}$) to the skin surface show that the number of ROS produced is dramatically reduced relative to the skin−UV filter control. After each UV filter remains on the skin surface for $t = 20$ min, the number of ROS generated increases, although it remains below the number generated in the control. By $t = 60$ min, the filters generate ROS above the control. The data show that when all three of the UV filters penetrate into the nucleated layers, the level of ROS increases above that produced naturally by epidermal chromophores under UV illumination.


*Keyword:* Free radicals

Sunscreens containing UV filters are recommended as part of safe-sun practices to reduce the effects of carcinogenic and photodamaging solar UV radiation. It is therefore an unsettling observation that increased sunscreen use has coincided with an increase in skin cancer. Most notably the incidence of melanoma has risen, although the relationship between the effects of sunscreens upon melanoma is hotly debated [1–6]. Complicating the traditional concept of photoprotection is our limited understanding of the photochemistry UV filters undergo in the skin. Of particular concern are photobiological reactions induced or mediated by reactive oxygen species (ROS). ROS are highly reactive derivatives of oxygen, including superoxide radical anion, hydroxyl radical, singlet oxygen ($^1O_2$), and hydrogen peroxide ($H_2O_2$), all of which can trigger further ROS generation [1,7]. To date the study of the effects of photoprotection molecules upon ROS production has been limited to a small number of solution-phase and in vitro experiments. *Para*-aminobenzoic acid (PABA) and 2-phenylbenzimidazle-5-sulfonic acid (PBSA) induce both $^1O_2$ and thymine-dimer formation, although the two have not been definitely correlated [8–14]. Solution-phase studies found that octylmethoxycinnamate (OMC), octocrylene (OC), and PABA all produce $^1O_2$ in phosphate-buffered saline (PBS) [8,13].

For photochemical reactions to be of concern, UV filters must penetrate through the stratum corneum, and recently reports have appeared that show such penetration can occur. Benzophenone-3 (B3) has been detected in human urine, with up to 1–2% of the applied amount estimated to be absorbed into the body [15,16]. B3 has also been detected in breast milk [16,17]. The amounts of B3, OMC, and octylsalicylate recovered from tape-stripped stratum corneum suggest that these UV filters penetrate into the epidermis [16,18].

These aforementioned studies have fueled concern that sunscreen molecules in the skin are at the very least incomplete photoprotectors against ROS and may even photogenerate highly destructive ROS. Understanding the relationship between UV filters and ROS is vital for understanding how one can fully protect oneself from damaging UV radiation. Traditionally, it has been impossible to collect data directly in the skin environment because of its opaque and heterogeneous nature. Recent advances in two-photon fluorescence microscopy have made it

*Abbreviations:* B3, benzophenones-3; DHR, dihydrorhodamine; OC, octocrylene; OMC, octylmethoxycinnamate; PABA, *para*-aminobenzoic acid; $ONOO^-$, peroxynitrite; R-123, rhodamine-123; ROS, reactive oxygen species; $^1O_2$, singlet oxygen; UV, ultraviolet; UVA, ultraviolet A radiation (320–450 nm); UVB, ultraviolet B radiation (280–320 nm).

* Corresponding author. Fax: +1 951 827 4713.
*E-mail address:* kerry.hanson@ucr.edu (K.M. Hanson).

0891-5849/$ - see front matter © 2006 Elsevier Inc. All rights reserved.
doi:10.1016/j.freeradbiomed.2006.06.011

possible to directly image fluorescent probes in skin at different epidermal depths [19–21]. In this paper, we use the fluorescent ROS indicator dihydrorhodamine (DHR) to study ROS levels in the nucleated epidermis after application of the UV filter B3, OC, or OMC. The goal of these experiments is to identify if, and under what conditions, UV filters produce highly reactive oxygen species in the skin.

## Materials and methods

### *Two-photon fluorescence microscope*

The two-photon fluorescence microscope has been described in detail [19,20]. In brief, an Nd:$YVO_4$ (Millenia; Spectra-Physics, Mountain View, CA, USA) pumped titanium:sapphire laser (Tsunami; Spectra-Physics) is coupled with a Zeiss Axiovert microscope (Maple Grove, MN, USA). The near-infrared (IR) laser light (785 nm) travels through the epifluorescence port of the microscope. A dichroic mirror (Chroma Technologies, Battleboro, NJ, USA) reflects the laser light and passes the green fluorescence to the photomultiplier (R3996; Hamamatsu, Bridgewater, NH, USA) positioned on the bottom port of the microscope. The laser power at the sample is 3 mW. Two filters (one 10 mm BG39 and one HG525/50M; Chroma Technologies) prevent residual IR and a fraction of the autofluorescence from reaching the PMT. Scanning mirrors and a 40× infinity corrected oil objective (F fluar, 1.3 NA; Zeiss) are used to image areas of 20 × 20 μm. A motorized *Z* stage (ASI, MultiScan-4, Lexington, KY, USA) is used to position the focal spot of the beam at different depths within the tissue. The SimFCS computer program (Laboratory for Fluorescence Dynamics, University of California at Irvine) is used for data acquisition and data analysis.

### *Sunscreen formulations and SPF*

The UV filters tested were OC, OMC, and B3 (ISP, Assonet, MA, USA). Water:oil emulsion formulae were created using 5% Finsolv solvent (Finetex, Elmwood Park, NJ, USA), 3% Sepigel-305 (Seppic, Fairfield, NJ, USA), 0.1% methylparaben preservative, UV filter, and water to 100 g. Each UV filter was tested at the maximum concentration approved by the FDA: OC—10%, OMC—7.5%, B3—6% of formulation. The in vitro SPF was experimentally determined for each formulation using Vitro-Skin (IMS, Inc., Milford, CT, USA). Vitro-Skin was cut into 6.2 × 9.0-cm rectangles and hydrated for 12 h in an IMS hydration chamber containing a 15% glycerin solution in water. One hundred microliters of sunscreen was applied to an area of 6.0 × 8.0 cm of VitroSkin with a positive pressure pipette and then rubbed over the surface with using a finger cot. The samples were allowed to dry for 15 min. Five measurements were taken over five different locations on the sample using a solar simulator (Model 16S; Solar Light Co., Glenside, PA, USA) as the irradiation source. An AIS Model DT-100 and Ocean Optics SD2000 fiber optic spectrometer (Dunedin, FL, USA) were used for light collection.

### *Tissue samples*

Two-photon fluorescence microscopy has been successfully used to image UV-induced ROS generation in both ex vivo skin and the epidermal skin model Epiderm (MatTek Corp., Ashland, MA, USA) [19,20]. Both types of tissues gave identical results for the experimental protocol used, but the epidermal model tissues provide the added advantage of reduced variability between samples as pigmentation, age, and body-site differences are nonexistent [21]. For this reason, we used the Epiderm tissues for the experiments in this paper. The skin is composed of normal human epidermal keratinocytes in a highly differentiated three-dimensional organotypic tissue. We have shown that Epiderm exhibits ROS-generating properties similar to those of ex vivo skin and thus is an excellent model for studying photoreactions of the skin [19,20].

### *Sample preparation and ROS detection through fluorescence*

Upon arrival each tissue insert was placed in a well of a six-well plate containing 0.9 ml of culture medium (MatTek Corp.). Tissues were incubated for 24 h (5% $CO_2$, 37°C) to bring to metabolic equilibrium, and the medium was replaced with fresh aliquots.

ROS were detected by the conversion of nonfluorescent DHR to fluorescent rhodamine-123 (R-123). DHR is oxidized to R-123 by reactions involving a variety of ROS, including $H_2O_2$, $^1O_2$, and $ONOO^-$ [19,22–25]. The photochemistry of DHR is complicated. For example, DHR may react with ROS other than those mentioned above, as well as undergo autoxidation [26]. In addition, R-123 may generate singlet oxygen itself, although its quantum yield is small (<0.03 in water) [27]. An aliquot of 100 μl dihydrorhodamine (15 μM DHR) in PBS was transferred to the surface of each tissue, which was then incubated for 1 h (5% $CO_2$, 37°C). DHR was removed from the surface, and the tissues were rinsed with three 100-μl aliquots of PBS.

Formulations were added to the surface of the skin using a positive-pressure pipette at 2 mg $cm^{-2}$—the dose recommended by the FDA [26, 28]. Each formulation was rubbed into the skin surface for 10 s using the tip of a glass rod. The tissues were incubated at 5% $CO_2$, 37°C for $t = 0$, 20, or 60 min. Forceps were used to gently remove each tissue from its insert and place it stratum corneum (SC)-side down upon filter paper (2 × 2 cm) wetted with PBS on a glass slide. A coverslip was secured over the tissue. Each sample was imaged before UV irradiation at 53 and 62 μm. Imaging through the basal layer avoids imaging through the highly scattering stratum corneum, which reduces image quality dramatically. Subsequently, each sample was flipped such that the SC was face-up onto a clean piece of PBS-wetted filter paper to allow for UV irradiation through the SC only. UV irradiation was provided by a solar simulator (Model 16S; Solar Light Co.) at a dose of 20 mJ $cm^{-2}$, which is equivalent to approximately 10 min of noonday summer sun in North America. Each tissue was flipped again onto a new piece of filter paper and reimaged on the two-photon microscope. Image areas were 20 × 20 μm. Nucleated layers were imaged at

depths $z = 53$ μm and $z = 62$ μm below the skin surface, well removed from the stratum corneum layer. These depths were selected because they are well within the nucleated epidermis. The fluorescence intensity of images acquired in the basal layer ($z = \sim 80$ μm) can be affected by the collagen-matrix foundation, which has a strong autofluorescence. At depths above 50 μm, the 20 × 20-μm images did not contain enough cells for cell-counting analysis to be statistically significant (data not shown). Two areas were imaged for each tissue sample, and each formulation was tested on two tissue samples.

*Cell-counting from images: statistical analysis and percentage ROS calculation*

The image analysis program (SimFCS) allows us to isolate each cell and record its average fluorescence intensity. Each image contained between 5 and 10 cells at depths $z = 62$ μm and $z = 53$ μm. Two areas per skin sample were analyzed, and two skin samples for each formulation were tested. For each data set, the results from a minimum of 48 cells were plotted in a histogram of frequency against R-123 intensity. The mean fluorescence intensity value was recorded ($I(z)$). The Student $t$ test was used to determine the statistical relevance of the data.

The number of ROS is proportional to the R-123 fluorescence. The enhancement of the ROS above the background level can be calculated as percentage ROS using Eq. (1) [19,20]:

$$\%-\mathrm{ROS}(z) = 100\left(\frac{I(z)_{UV-filter}}{I(z)_{control}}\right) \quad (1)$$

$I(z)_{\mathrm{control}}$ is the mean fluorescence intensity obtained from the histograms from the control data (skin − UV filter) and represents the number of ROS that are generated by intrinsic chromophores in the skin at the UV irradiance used (200 mJ $\mathrm{cm}^{-2}$). $I(z)_{\mathrm{UV\text{-}filter}}$ is the mean fluorescence intensity from the histograms of B3, OC, or OMS. A value of 100% ROS is equivalent to the natural level of ROS that the imaged nucleated keratinocytes generate in the absence of the sunscreen molecules.

## Results

The SPF for each formulation was as follows: B3, 8 ± 3; OC, 6 ± 2; OMC, 6 ± 1. UV filters in the absence of the ROS probe DHR do not exhibit increased fluorescence after UV irradiation of the skin (200 mJ $\mathrm{cm}^{-2}$). As a control experiment, Fig. 1 shows the basal layer of skin applied with the OC formulation before (Fig. 1a) and after (Fig. 1b) UV irradiation by the solar simulator. The background autofluorescence level of the cells is shown in Fig. 1c. No increase in intensity was detected after UV irradiation. Identical results were detected for all formulations tested (data not shown). Thus, all fluorescence detected in the skin for each formulation tested results from the conversion of DHR to R-123. R-123 can be formed both after the reaction of DHR with ROS (i.e., $H_2O_2$, $^1O_2$, and $ONOO^-$) [19,22–25] and through DHR autoxidation [26]. In addition, although its quantum yield is small, R-123 may generate singlet oxygen itself [27]. The images we acquired cannot distinguish between the mechanisms that generate R-123 and ROS. However, as we show below, our time-course data act as an inherent control. We saw an increase in fluorescence intensity with the amount of time the UV filters remained on the skin relative to samples in which only DHR/R-123 were present. This strongly suggests the UV filters themselves generate ROS that in turn react with DHR. If the UV filters did not generate ROS and/or autoxidation was the dominant photochemical pathway, then we would not see any increase in the R-123 fluorescence with incubation time/UV-filter penetration. Thus, the images displayed herein show that under these experimental conditions, DHR does react with ROS in the skin, even if some autoxidation may occur concurrently.

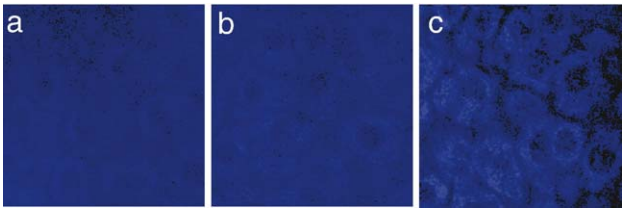


Fig. 1. Autofluorescence intensity images of skin incubated with OC (in the absence of DHR) (a) before and (b) after 20 mJ $\mathrm{cms}^{-2}$ UVB–A. (c) Image of skin applied with the control, incubated for $t = 60$ min, before UV irradiation.

Images of skin ($z = 62$ μm) taken immediately after application with B3, OC, or OMC to the skin's surface ($t = 0$ min) and after subsequent irradiation with 200 mJ $\mathrm{cm}^{-2}$ UVB–UVA show a dramatic reduction in R-123 fluorescence relative to the control (skin − UV filter) (Fig. 2). All images are displayed using the same intensity scale, in which regions of bright red and yellow indicate high fluorescence signal. R-123 fluorescence was predominately detected from the cytoplasm of the keratinocytes of each epidermal layer, which is consistent with data collected previously on Epiderm and ex vivo tissues and is attributed to ROS generation from intrinsic chromophores (i.e., NADH, riboflavin, mitochondria) [19,20,29–31]. Regions of dark blue in the nuclei and extracellular spaces indicate low fluorescence signal equivalent to typical autofluorescence levels as displayed in Figs. 1a–1c. At $t = 20$ min, after each UV filter remained on the surface for 20 min, images acquired post-UV irradiation still show a decrease in R-123 fluorescence relative to the control images (skin − UV filter). However, as Fig. 2 shows, more cytoplasmic R-123 fluorescence was detected compared to the $t = 0$ images for each UV filter tested. Cytoplasmic R-123 fluorescence continued to increase until at $t = 60$ min, when the UV filters had been on the skin for 1 h, the post-UV images for OC, OMC, and B3 show more intracellular R-123 fluorescence than either the control or the $t = 0$ and $t = 20$ min images. The same trend was seen for images acquired at $z = 53$ μm (data not shown), in which the R-123 fluorescence of the nucleated cells at this depth gradually increased, being the least at $t = 0$ min and the greatest, and above that of the corresponding control, at $t = 60$ min.

The images show that a direct correlation exists between R-123 fluorescence intensity and the length of time a UV filter

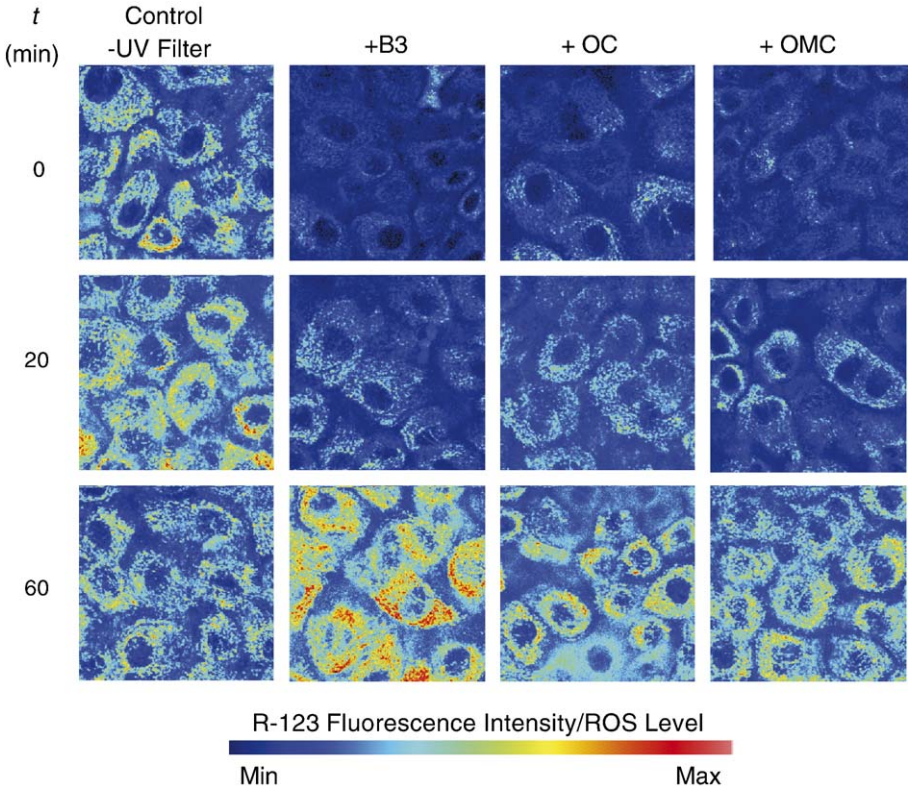


Fig. 2. Two-photon fluorescence intensity images of R-123 fluorescence ($z = 62$ μm) in the skin after 20 mJ cm$^{-2}$ UVB–UVA irradiation. A comparison "before UV" image is displayed in Fig. 1c. All images are shown using the same intensity scale, in which red indicates the maximum fluorescence detected and blue correlates with intensities similar to those emitted by autofluorescence. Each UV filter was left on the skin surface for $t = 0$, 20, or 60 min before the images were acquired. Each image is 20 × 20 μm.

remains on the skin's surface (Fig. 2). In order to quantify the effect of incubation time upon R-123 fluorescence, and thus ROS levels, in the nucleated layers, we had to account for variations in tissue morphology, which can lead to different numbers of cells within different observation windows. For example, if a tissue section happens to have few cells, even if those cells show a high level of fluorescence the total fluorescence level of the image can be too low. To avoid this, we analyzed the average fluorescence levels for individual cells in the images and tabulated the results in a manner similar to what is done in cell cytometry experiments. As described under Materials and methods, a histogram of frequency vs R-123 intensity was created for each formulation tested at each incubation time (Fig. 3). Each histogram contains all cells counted at $z = 53$ μm and $z = 62$ μm. A broad distribution is seen in the data, which are typical for fluorescence collected by two-photon microscopy in the skin [19–21]. Even using the skin model tissue, we have found that the heterogeneous environment consistently yields broad distributions, which can be attributed to differences in dye penetration, ROS production between cells, ROS production between skin samples, and chromophore content differences between cells within a sample. These differences are greater for ex vivo skin.

The statistical significance of the histograms can be evaluated using a one-way ANOVA using the Bonferroni criterion to judge whether a given sunscreen histogram is statistically different from the control at a given time. For each comparison, we found that the means were statistically different ($p < 0.008$ for a 95% certainty level), with the exception of OC vs control at $t = 60$ min. The less conservative Student $t$ test calculates that these same data all have a greater than 95% probability of being statistically unique relative to the control sample. Each mean value is identified on each histogram by an arrow and the corresponding value is listed in Table 1. As the time each UV filter remained on the skin's surface increased, a gradual shift in the mean fluorescence intensity was seen in the nucleated layers. At $t = 0$ min, when images were acquired immediately after application of the formulations, the ROS values were the lowest, illustrating how a sunscreen should work—the UV filter remained on the skin surface, attenuating UV in the stratum corneum before it could reach into the nucleated layers. At $t = 20$ min the number of ROS increased for each UV filter tested. This indicates that at the very least the UV filters have lost efficacy in protecting the nucleated epidermal keratinocytes from UV-induced ROS generation by intrinsic chromophores in the cells. After $t = 60$ min, the mean fluorescence intensity of each UV filter increased above that of the cream-only control, with B3 yielding the greatest increase. The time evolution of the increased fluorescence is illustrated graphically in Fig. 4, which shows the time-dependent change in percentage ROS (calculated using the mean fluorescence intensity values and Eq. (1)) for each of the three UV filters tested. In other words, when the filters had remained on the surface for 1 h before images were acquired, each ROS value had increased above the number of

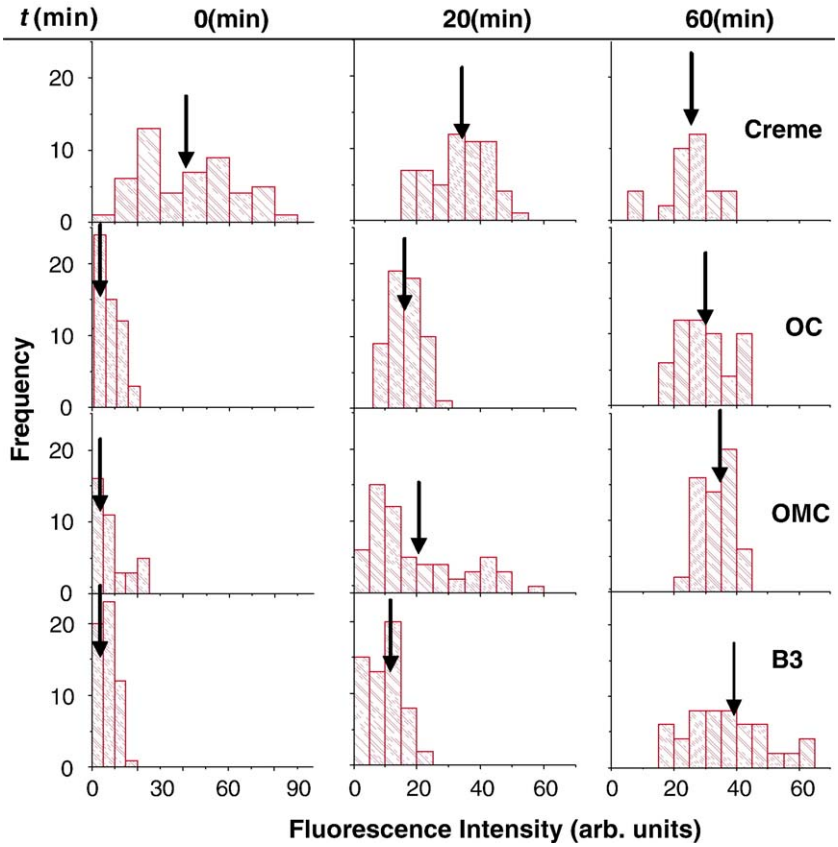


Fig. 3. Histogram data of the R-123 fluorescence intensity for counted cells at depths $z = 53$ and 62 μm. The arrows indicate the calculated mean (one-way ANOVA, post hoc Bonferroni test ($p < 0.008$) for each UV filter vs control comparison). Histograms are displayed of data acquired at $t = 0$, 20, or 60 min post-application of each formulation. Each mean intensity has a greater than 95% probability (Student $t$ test) of being greater than that of the control mean; however, one-way ANOVA with post hoc Bonferroni analysis indicates that at $t = 60$ min the mean of OC is not statistically different from that of the control. Mean and $p$ values are listed in Table 1.

ROS generated by naturally occurring epidermal chromophores. Note that part of this increase is due to the fact that the mean control fluorescence level is decreasing with time. This may be the result of the penetration of parabens into the skin. Nakagawa et al. found that parabens (0.1–0.5 mM), like 12,13-alkyl benzoate (Finsolv) used in our formulation, induce cell death by activating the mitochondrial permeability transition, in turn causing ATP depletion [32]. We used 5% Finsolv and 1% methylparaben preservative (total concentration ~200 mM) that, upon penetration into the skin, may have reduced mitochondrial activity [32]. Analogous to the results of Nakagawa et al., the control data may be decreasing in mean fluorescence intensity with cream incubation time simply because as $t$ increases, more paraben penetrates and yields a reduction in cell respiration and ROS sources.

The data in Figs. 3 and 4 result strongly suggest that the B3, OC, and OMC themselves generated ROS in the nucleated keratinocytes imaged. Because the only ROS known to react with DHR are $H_2O_2$, $^1O_2$, and $ONOO^-$, it is possible that other ROS that do not react with DHR are also present [19,22–25]. Thus, the amount of fluorescence detected represents a minimum level, in that both intrinsic chromophores and the UV filters may generate ROS that do not react with DHR and thus are not represented in the images displayed herein.

Table 1
Mean R-123 fluorescence intensity calculated from the corresponding histogram of counted cells at $z = 52$ and 63 μm

| Sample | Mean intensity ($p$)[a] | | |
|---|---|---|---|
| | $t = 0$ min | $t = 20$ min | $t = 60$ min |
| Control | 41.9 | 33.0 | 25.3 |
| B3 | 4.4 (0) | 7.4 (0) | 41.4 (<0.00001) |
| OC | 5.1 (0) | 16.0 (0) | 29.4 (0.02) |
| OMC | 3.1 (0) | 19.2 (<0.00001) | 33.6 (<0.00001) |

[a] Values of $p$ were calculated based upon the one-way ANOVA, post hoc Bonferroni analysis (significance level 0.008) in which each UV filter was compared to the control.

## Discussion

Our experimental data show the effects of sunscreen molecules upon UV-induced ROS generation in nucleated epidermis. The surprising result is that the UV filters applied to the skin surface not only lose their screening capability after a period of incubation, but also may lead to enhanced ROS generation in nucleated epidermis through photogeneration. Such a scenario requires two things: first, that the sunscreen molecules are able to penetrate beyond the stratum corneum and second, that they can act as sources for ROS generation. Both phenomena have precedence in the literature.

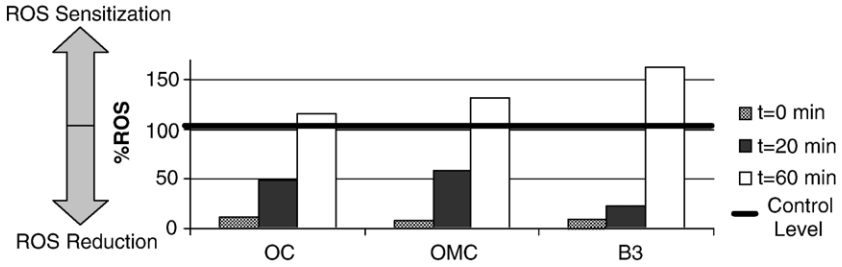


Fig. 4. %ROS values of the UV filters based upon the mean intensity values in Table 1 (Eq. (1)). 100% ROS is equivalent to the number of ROS generated by naturally occurring chromophores in the nucleated keratinocytes for skin absent any UV filter (control images) after irradiation by 20 mJ $cm^{-2}$. %ROS values below 100% indicate a reduction in the level of ROS produced in these layers. %ROS values above 100% indicate an increase in the level of ROS produced above that produced naturally for the same UVB–UVA irradiance.

We first focus on sunscreen penetration. There are several recent reports which find that UV filters can penetrate the stratum corneum and solution-phase studies showing some UV filters can generate ROS. Our data show that $\%ROS_{OC} < \%ROS_{OMC} < \%ROS_{B3}$, which is consistent with the reported and predicted penetration properties of these UV filters. Of the molecules we tested, B3 and OMC have previously been reported to penetrate through the stratum corneum [15–18]. The structural similarities between OMC and OC suggest that OC should penetrate as well. Their lipophilic side chains should reduce penetration through the lipid-rich stratum corneum compared to B3, which is the least lipophilic of the three and thus penetrates more easily [16]. In addition, Watkinson et al. developed a theory predicting penetration of UV filters, which our data follow [16,33]. The fluorescence data show that the trend in the amount of ROS generated by each organic UV filter in the nucleated layers is consistent with the relationship

$$k \propto M^{-1/3}, \tag{2}$$

where $k$ is the rate constant for molecular transport through the stratum corneum and $M$ is the UV-filter molecular weight. It should be noted that this is a simplified relationship, in which the rate of penetration through the skin can be affected by the formulation hosting the UV-filter [16,18,33]. Eq. (2) predicts that $k_{OC} < k_{OMC} < k_{B3}$. In our experiments, we do not directly measure $k$, but if we assume that a small amount of sunscreen does diffuse into the epidermal layers, the amount present after a period of time should be directly proportional to the rate defined in Eq. (2) and thus directly proportional to $M^{-1/3}$. In Fig. 5 we plot the amount of increased R-123 signal versus $M^{-1/3}$ for the three sunscreens examined here. Even though there are only three points, these data points are clearly consistent with the linear dependence predicted by Eq. (2). The statistical analysis showing that at $t = 60$ min OC had the least difference in fluorescence compared to the control ($p = 0.02$ for $\alpha = 0.008$) is consistent with the penetration characteristics of OC. Fig. 5 shows that the enhancement in ROS levels is consistent with what would be expected if they were due to sunscreen penetration through the skin. Ideally, the ROS levels at different depths would be correlated with the amount of sunscreen present, which would be determined independently. Experimentally, however, it is very difficult to quantify the concentration of sunscreen at the different epidermal depths. The traditional method of tape-stripping is strata-nonspecific, providing only a bulk value for the upper and lower epidermal regions. We also attempted multiphoton fluorescence microscopy of the UV filters in the skin; however, their low fluorescence quantum yield values prohibited data collection.

Once the sunscreen molecules have reached the lower layers of the skin, the next question is whether they are capable of generating ROS. Recent solution-phase experiments have demonstrated that OC and OMC produce ROS. OMC and OC generate $^1O_2$ as determined by fufuryl alcohol consumption in sodium phosphate buffer [9,13]. The same study did not find B3 to produce $^1O_2$; however, it is known that the solvent affects the lifetime of the B3 triplet state needed for energy transfer to $O_2$ and it is possible that the highly lipophilic environment of the cell interior may enhance this lifetime [13,34]. The mechanism by which B3, OC, and OMC generate $^1O_2$ is not fully understood. However, as each UV filter tested has an available triplet state capable of energy transfer to $O_2$, $^1O_2$ may be generated through triplet energy transfer, if as in the case of OMC ($E_T = 239$ kJ $mol^{-1}$) the triplet state energy is greater than that of singlet oxygen (94 kJ $mol^{-1}$). Singlet oxygen can lead to the formation of superoxide radical anion, which in turn may generate hydrogen peroxide, which in the presence of biological levels of $Fe^{2+}$ can generate hydroxyl radical through the Fenton reaction [1].

The data in this paper lead to a conclusion different from that of earlier experiments on the role of OMC in ROS generation.

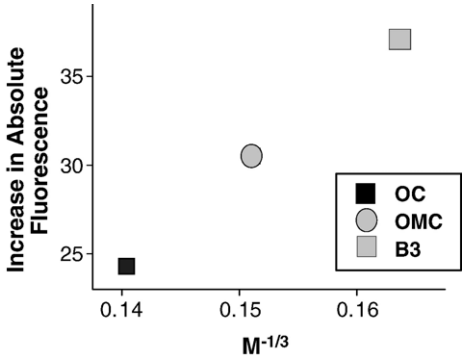


Fig. 5. Graph of the increase in fluorescence signal ($(t = 60$ min$) - (t = 0$ min$)$) against $M^{-1/3}$, where $M$ is equivalent to the molecular weight of B3, OC, or OMC. The lowest molecular weight UV filter, B3, yields the greatest fluorescence signal due to greater penetration into the nucleated epidermal layers.

We have previously shown that a formulation containing OMC and avobenzone and an incubation period of $t=3$ h reduced ROS levels in ex vivo skin. However, several differences exist between the two experiments. First, the tissue used previously was ex vivo breast and facial tissue kept at 4°C, whose barrier properties may be different from those of the epidermal model tissue at room temperature. Second, the UV light source used herein was a solar simulator emitting both UVB and UVA radiation, unlike the UVB fluorescent bulbs used in the previous experiment, which have a sharp peak near 300 nm. The number of ROS generated may be affected by wavelength. Finally, it should be emphasized that differences between the formulations used in the two experiments could have dramatically affected penetration [16,18].

## Conclusions

The data discussed herein show that if the UV filters B3, OC, and OMC penetrate through the stratum corneum, they can generate highly reactive oxygen species in the cytoplasm of the nucleated keratinocytes in the epidermis. Clearly, determining what, if any, type of damage is done by ROS generated by UV filters needs to be explored. The simple oil:water emulsifier formulation used in these experiments may have allowed more of each UV filter to penetrate than a more advanced formulation that could retain the filters on the skin's surface. Thus, whether formulation vehicles, or antioxidants, could affect UV filter-sensitized ROS generation would be of great interest to understand in order to possibly improve sunscreens. Even with some sunscreen penetration, if UV attenuation is significant at the skin surface then UV filter sensitization of ROS in the nucleated layers would be minimized if not negligible. Thus, correct application, and reapplication, of sunscreens may be necessary to limit the effects of any UV-filter production of ROS.

## Acknowledgments

Patrick Hayden, Ph.D., and MatTek Corp. (Ashland, MA, USA) generously provided all Epiderm tissues and helpful discussions. C.J.B. acknowledges support from the National Science Foundation, Grant MCB-0344719. The LFD is supported by NIH Grant RR03155.

## References

[1] Gasparro, F. P. New perspectives in sunscreen photobiology. In: Gasparro, F. P., ed. *Molecular, cellular and physiological aspects*. Berlin: Springer-Verlag; 1997:177–186.

[2] Garland, C. F.; Garland, F. C.; Gorham, E. D. Rising trends in melanoma: an hypothesis concerning effectiveness. *Ann. Epidemiol.* **3:**103–110; 1993.

[3] Autier, P.; Dore, J. F.; Schifflers, E.; Cesarini, J. P.; Bollaerts, A.; Koelmel, K. F.; Gefeller, O.; Liabeuf, A.; Lejeune, F.; Lienard, D. Melanoma and use of sunscreens: an EORTC case–control study in Germany, Belgium and France. *Int. J. Cancer* **61:**749–755; 1995.

[4] Wartha Wright, M.; Wright, S. T.; Wagner, R. F. Mechanisms of sunscreen failure. *J. Am. Acad. Dermatol.* **44:**781–784; 2001.

[5] Stern, R. S.; Weinstein, M. C.; Baker, S. G. Risk reduction for nonmelanoma skin cancer with childhood sunscreen use. *Arch. Dermatol.* **122:**537–545; 1986.

[6] Bastuji-Garin, S.; Diepgen, T. L. Cutaneous malignant melanoma, sun exposure and sunscreen use: epidemiological evidence. *Br. J. Dermatol.* **146:**24–30; 2002.

[7] Mylonas, C.; Kouretas, D. Lipid peroxidation and tissue damage. *In Vivo* **13:**295–309; 1999.

[8] Allen, J. M.; Gossett, C. J.; Allen, S. K. Photochemical formation of singlet molecular oxygen in illuminated aqueous solutions of PABA. *J. Photochem. Photobiol.* **32:**33–37; 1996.

[9] Allen, J. M.; Gossett, C. J.; Allen, S. K. Photochemical formation of singlet molecular oxygen in illuminated aqueous solutions of several commercially available sunscreen active ingredients. *Chem. Res. Toxicol.* **9:**605–609; 1996.

[10] Aliwell, S. R.; Martineigh, B. S.; Salter, L. F. Photoproducts formed by near-UV irradiation of thymine in the presence of PABA. *J. Photochem. Photobiol. A Chem.* **83:**223–228; 1994.

[11] Sutherland, B. M. PABA acid-sunlamp sensitization of pyrimidine dimer formation and transformation in human cells. *Photochem. Photobiol.* **36:**95–97; 1982.

[12] Hu, M.-L.; Chen, Y.-K.; Chen, L.-C.; Sano, M. PABA scavenges reactive oxygen species and protects DNA against UV and free radical damage. *J. Nutr. Biochem.* **6:**504–508; 1995.

[13] Cantrell, A.; McGarvery, D. J.; Truscott, T. G. Photochemical and photophysical properties of sunscreens. In: Giacomoni P. U. (ed.), *Sun protection in man*. Amsterdam: Elsevier; 2001; 495–519.

[14] Inbaraj, J. J.; Bilski, P.; Chignell, C. F. Photophysical and photochemical studies of 2-phenylbenzimidazole and UVB sunscreen 2-phenylbenzimidazole-5-sulfonic acid. *Photochem. Photobiol.* **75:**107–116; 2002.

[15] Hayden, C. G. J.; Roberts, M. S.; Benson, H. A. E. Systemic absorption of sunscreen after topical application. *Lancet* **350:**863–864; 1997.

[16] Walters, K. A.; Roberts, M. S. Percutaneous absorption of sunscreens. In: Bronaugh, R. L.; Maibach, H.I. eds. *Topical absorption of dermatological products*. New York: Dekker; 2002:465–481.

[17] Hany, J.; Nagel, R. Detection of sunscreen agents in human breast milk. *Dtsch. Lebensm. Rundsch.* **91:**341–345; 1995.

[18] Treffel, P.; Gabard, B. Skin penetration and SPF of ultraviolet filters from two vehicles. *Pharm. Res.* **13:**770–774; 1996.

[19] Hanson, K. M.; Clegg, R. M. Observation and quantification of UV-induced ROS generation in *ex vivo* human skin. *Photochem. Photobiol.* **76:**57–63; 2002.

[20] Hanson, K. M.; Clegg, R. M. Two-photon fluorescence imaging and ROS detection within the epidermis. In: Turksen, K., ed. *Methods in molecular biology: epidermal cells, methods and protocols*. Clifton, NJ: Humana Press; 2003:413–421.

[21] Hanson, K. M.; Clegg, R. M. Sunscreen and antioxidant effects upon UV-induced ROS in human skin: a two-photon fluorescence microscopy study. *J. Cosmet. Sci.* **54:**589–598; 2003.

[22] Henderson, L. M.; Chappell, J. B. Dihydrorhodamine 123: a fluorescent probe for superoxide generation? *Eur. J. Biochem.* **217:**973; 1993.

[23] Royall, J. A.; Ischiropoulos, H. Evaluation of 2′,7′-dichlorofluorescin and dihydrorhodamine 123 as fluorescent probes for intracellular $H_2O_2$ in cultured endothelial cells. *Arch. Biochem. Biophys.* **302:**348–355; 1993.

[24] Kooy, N. W.; Royall, J. A.; Ischiropoulos, H.; Beckman, J. S. Peroxynitrite-mediated oxidation of dihydrorhodamine 123. *Free Radic. Biol. Med.* **16:**149–156; 1994.

[25] Crow, J. P.; Beckman, J. S.; McCord, J. M. Sensitivity of the essential zinc-thiolate moiety of yeast alcohol dehydrogenase to hypochlorite and peroxynitrite. *Biochemistry* **34:**3544–3552; 1995.

[26] Chignell, C. F.; Sik, R. H. A photochemical study of cells loaded with 2′,7′-dichlorofluorescein: implications for the detection of reactive oxygen species generated during UVA radiation. *Free Radic. Biol. Med.* **34:**1029–1034; 2003.

[27] Butorina, D. N.; Krasnovskii, A. A.; Savvina, L. P.; Kuznetsova, N. A. Bromorhodamines as efficient photosensitizers in the formation of singlet molecular oxygen in aqueous and ethanolic solutions. *Russ. J. Phys. Chem.* **79:**791–794; 2005.

[28] Food and Drug Administration, Final sunscreen monograph. *Fed. Reg.* **64:**27666–27693; 1999.

[29] Jurkiewicz, B. A.; Buettner, G. R. EPR detection of free radicals in UV-irradiated skin: mouse versus human. *Photochem. Photobiol.* **64:**918–922; 1996.

[30] Cunningham, M. L.; Krinsky, N. I.; Giovanazzi, S. M.; Peak, M. J. Superoxide anion is generated from cellular metabolites by solar radiation and its components. *J. Free Radic. Biol. Med.* **1:**381–385; 1985.

[31] Peak, M. J.; Peak, J. G. Solar-UV-induced damage to DNA. *Photodermatology* **6:**1–15; 1989.

[32] Nakagawa, Y.; Moore, G. Role of mitochondrial membrane permeability transition in *p*-hydroxybenzoate ester-induced cytotoxicity in rat hepatocytes. *Biochem. Pharmacol.* **58:**811–816; 1999.

[33] Watkinson, A. C.; Brain, K. R.; Walters, K. A.; Hadgraft, J. Prediction of the percutaneous penetration of UV filters used in sunscreen formulations. *Int. J. Cosmet. Sci.* **14:**265–275; 1992.

[34] Lamola, A. A.; Sharp, L. J. Environmental effects on the excited states of *o*-hydroxy aromatic carbonyl compounds. *J. Phys. Chem.* **70:**2634–2638; 1966.